# Removal of 1,2-Dichloroethane from Aqueous Solutions with Novel Composite Polydimethylsiloxane Pervaporation Membranes

**Liang Liang,[1] James M. Dickson,[2] Zhen Zhu,[3] Jianxiong Jiang,[4] Michael A. Brook[4]**

[1]*eVionyx Inc., 6 Skyline Drive, Hawthorne, New York 10532*
[2]*Department of Chemical Engineering, McMaster University, Hamilton, Canada L8S 4L7*
[3]*Buffalo Research Laboratory, Honeywell, 20 Peabody Street, Buffalo, New York 14210*
[4]*Department of Chemistry, McMaster University, Hamilton, Canada L8S 4M1*

Received 26 December 2003; accepted 9 December 2004
DOI 10.1002/app.21752
Published online in Wiley InterScience (www.interscience.wiley.com).

**ABSTRACT:** Composite pervaporation membranes were prepared by the crosslinking of H-terminated oligosilylstyrene (oligo-$SiH_3$) and vinyl-terminated polydimethylsiloxane (vinyl-PDMS) on the surface of polysulfone ultrafiltration membranes. The morphology of the composite pervaporation membranes were investigated through changes in the mass ratio of oligo-$SiH_3$ to vinyl-PDMS. The pervaporation of crosslinked polydimethylsiloxane composite membranes was evaluated by the removal of 1,2-dichloroethane (1,2-DCE) from dilute aqueous solutions with different downstream pressures, feed temperatures, feed concentrations, and top layer thicknesses. A low feed flow rate, corresponding to a Reynolds number of 97, was maintained during the entire process. The separation factor of 1,2-DCE was 600–4300, and the permeation rate of 1,2-DCE was 0.4–15 g/m$^2$ h; they depended on the operating conditions and the compositions of the membranes. © 2005 Wiley Periodicals, Inc. J Appl Polym Sci 98: 1477–1491, 2005

**Key words:** polysiloxanes; separation techniques; crosslinking

## INTRODUCTION

Two challenges should be addressed during the process of developing pervaporation membranes: membrane selectivity and membrane strength and chemical stability. The former determines what kinds of chemical species can be separated. The latter represents the lifetime of membranes. Although numerous polymer membranes have been used in pervaporation,[1–8] much effort has been expended on developing polydimethylsiloxane (PDMS) membranes. This is because PDMS membranes have the highly desired ability to remove volatile organic compounds (VOCs) from aqueous solutions, and this can make a significant contribution to environmental protection.[9–19] However, PDMS itself has poor mechanical strength;[20] in particular, pure PDMS is a viscous liquid at room temperature, and so its application as a pervaporation membrane is restricted. To improve the mechanical strength, PDMS membranes have been modified by block copolymers, graft copolymers, crosslinking networks, and even nanomaterials.[21–29] Among these methods, crosslinking PDMS is one of the most effective for enhancing the mechanical strength of PDMS membranes without the loss of the function of pervaporation.

We know that $\beta$-trichlorosilylstyrene (TCSS) as an oligomer can efficiently react with H-terminated PDMS to generate crosslinked PDMS.[30] Because of the rigid silylstyrene structure and more hydrophobic characteristics of TCSS chains, both the strength and selectivity of final PDMS membranes to hydrophobic chemicals are expected to increase.[31] A previous study disclosed the pervaporation characteristics of crosslinked PDMS membranes prepared by OH-terminated PDMS and TCSS.[32] The membranes showed a higher permeation rate of 1,2-dichloroethane (1,2-DCE) and excellent selectivity. Unfortunately, the membranes were damaged by hydrochloric acid (HCl), which was generated as a byproduct during the reaction of OH-terminated PDMS and TCSS. In addition, moisture in air affected the curing rate of OH-terminated PDMS and TCSS, and this resulted in membranes that were thermodynamically unstable. Membranes with nonuniform crosslinking density were formed because the moisture in the curing environment was difficult to control. To eliminate the effects of HCl and moisture, H-terminated oligosilylsty-

*Correspondence to:* L. Liang (liang_liang@verizon.net).
Contract grant sponsor: Ministry of Economic Development and Trade (Ontario, Canada).
Contract grant sponsor: National Science and Technology Board of Singapore.

rene (oligo-$SiH_3$) was developed. Crosslinked PDMS membranes were synthesized from oligo-$SiH_3$ and vinyl-terminated polydimethylsiloxane (vinyl-PDMS).[33] With this approach, there was no HCl as a byproduct, and the prepared PDMS membranes were quite durable. Furthermore, the prepared PDMS membranes demonstrated excellent performance when used to separate various VOCs, including 1,2-DCE, from aqueous solutions by pervaporation.[34] However, the performances of membranes prepared from oligo-$SiH_3$ and vinyl-PDMS have not been evaluated in detail by the combination of the membrane composition and fabrication procedure. The separation of 1,2-DCE has not been explored by the relationship between the intrinsic properties of the membranes and the pervaporation conditions. We are interested in the pervaporation of 1,2-DCE because 1,2-DCE is a toxic organic compound with relatively high water solubility[35] and the ability to migrate in soil.[36] Moreover, 1,2-DCE is frequently used as a chemical intermediate, solvent, and lead scavenger in gasoline.[37] Recently, interest in 1,2-DCE contamination increased when 1,2-DCE was detected in groundwater in many areas.[38,39] Groundwater often moves slowly, and the residence time of 1,2-DCE can range from years to centuries. Therefore, the potential pollution from 1,2-DCE to human beings and environments is long-term. On the basis of our knowledge, few studies had been conducted on the pervaporation of 1,2-DCE, in comparison with numerous investigations on other chlorinated organic compounds such as chloroform, trichloroethylene, trichloroethane, and dichloro methane.[40–45] This study improves our knowledge of the separation of 1,2-DCE by pervaporation. Meanwhile, we investigated a lower flow rate of the feed solution through the pervaporation cell; it corresponded to a Reynolds number of 97. In this case, higher mass-transfer resistance through the membranes can be expected because there is a significant effect from the boundary layer.[45] However, the cost of separation could be dramatically reduced if a lower flow rate is maintained.[46] This study should also help us to understand the characteristics of pervaporation with economical operating conditions.

## EXPERIMENTAL

### Materials

Vinyl-PDMS (Hülser-Petrach, Sussex, NJ), a platinum divinyltetramethyldisiloxane complex (Pt catalyst; 3% in toluene; Gelest, Tullytown, PA), hexane (99%; Fisher), 1,2-DCE (99%; Aldrich, Milwaukee, WI), $LiAlH_4$ (powder; 95%; Aldrich), trichlorosilane (99%; Aldrich), trifluoromethanesulfuric acid ($CF_3SO_3H$; 99%; Aldrich), and octamethylcyclotetrasiloxane (99%; Aldrich) were used without purification. Phenylacetylene (98%; Aldrich) was distilled before it was used. The deionized water was used in all experiments. Polysulfone (PSF) ultrafiltration membranes 175 $\mu$m thick (U.S. Filter, Warrendale, PA) and nonwoven polypropylene as a support layer were used. The PSF membranes could cut off a dextran with a molecular weight of 100,000. The PSF membranes were purified by being soaked in isopropyl alcohol overnight for the removal of residual chemicals inside the membranes. Then, the PSF membranes were exposed in a hood at room temperature for complete drying.

### Synthesis of oligo-$SiH_3$

The synthesis of oligo-$SiH_3$ was reported in a previous study,[33,34] and the multiple synthetic steps are schematically shown in Figure 1. The synthetic method can be summarized as follows: Trichlorosilane (370 g) was added to phenylacetylene (636 g). $H_2PtCl_6$ (0.8 mL, 0.3% in isopropyl alcohol) was added to the solution at 0°C (ice bath) with stirring. The solution was warmed to room temperature with stirring. After the distillation of excess trichlorosilane, pure TCSS was produced by vacuum distillation (92°C at 12 mmHg). The oligomerization of TCSS was carried out by the mixing of TCSS (43.3 g) with $CDCl_3$ (3.0 mL), and then $CF_3SO_3H$ (1.2 mL) was added to the solution at −15°C. The temperature was allowed to warm to room temperature, and the reaction was continued for 2 h more. To extend the length of the functional groups to speed up the crosslinking, octamethylcyclotetrasiloxane {[—$Si(CH_3)_2O$—]$_4$, 3 equiv/$SiCl_3$} was added to the reaction system at 0°C, and the solution was warmed to room temperature over 2 h. Then, the solution was heated to 75°C for 24 h, and the reaction was continued for an additional 48 h. This process allowed the insertion of octamethylcyclotetrasiloxane between —Si and —Cl atoms in the —$SiCl_3$ end groups. Finally, the trichlorosilylstyrene oligomer (124.1 g) was added to 150 mL of ether, and 3.9 g of $LiAlH_4$ was added to 80 mL of ether under an $N_2$ atmosphere. The solution of the trichlorosilylstyrene oligomer was added dropwise to the $LiAlH_4$ suspension with stirring. The reaction mixture was warmed to room temperature for at least 4 h. The supernatant was carefully decanted from the reaction solids. The solids were then washed with ether, and the collected solutions were washed and extracted with $H_2O$/ether until the pH value of the final solution was close to 6.5. After drying completely, oligo-$SiH_3$ as a clear oil was obtained by the evaporation of the solvents of the organic phase at temperatures up to 100°C for 2–3 h *in vacuo*. The yield of terminated oligosilylstyrene was approximately 84%.

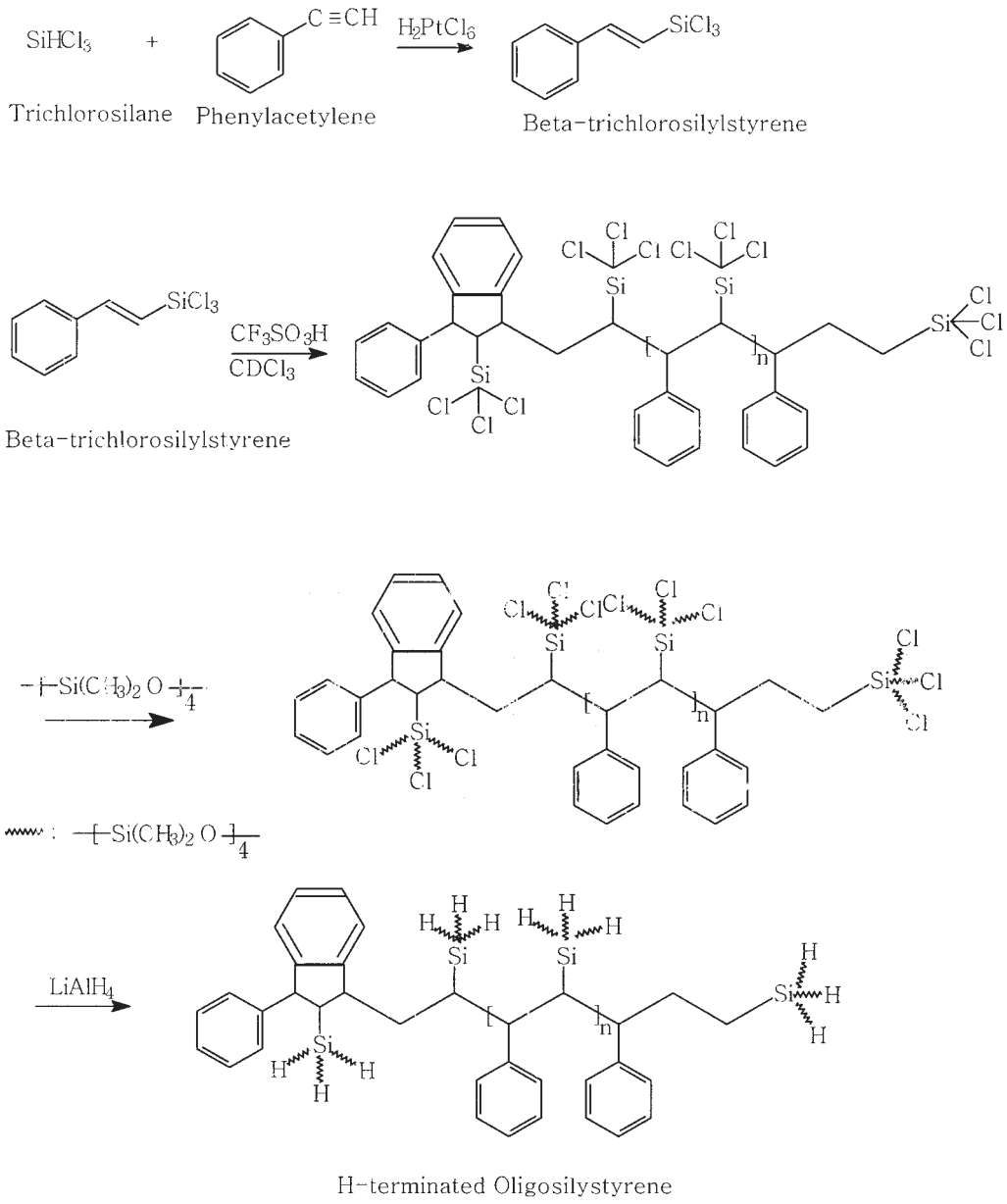


**Figure 1** Schematic illustration of the synthetic route for oligo-$SiH_3$.

### Preparation of crosslinked PDMS composite membranes

The formulations used to prepare the composite membranes are listed in Table I. A typical preparation procedure can be briefly described as follows: A vinyl-PDMS solution was prepared by the dissolution of 1.0 g of vinyl-PDMS and 0.2 mL of Pt catalyst in 5 mL of hexane at room temperature with stirring. An oligo-$SiH_3$ solution was prepared by the dissolution of 0.2 g of oligo-$SiH_3$ in 1 mL of hexane at room temperature with stirring. We mixed two solutions for 0.5 h at room temperature. Finally, the mixed solution was poured onto the surface of a PSF membrane that was clamped to a cell with a diameter of 90 mm. The solvent was allowed to evaporate at room temperature overnight. The crosslinked PDMS gel, as the top layer of the composite membrane, was generated on the surface of the PSF membrane by the reaction of vinyl groups at the PDMS chains and H atoms at oligo-$SiH_3$ chains, as shown schematically in Figure 2. To achieve complete

**TABLE I**
**Compositions of the Casting Solutions for the Crosslinked PDMS Composite Membranes**

| Oligo-$SiH_3$/vinyl-PDMS (mass ratio) | Oligo-$SiH_3$ (g) | Vinyl-PDMS (g) | Hexane (mL) |
|---|---|---|---|
| 0.5 | 0.4 | 0.8 | 6 |
| 0.2 | 0.2 | 1.0 | 6 |
| 0.1 | 0.1 | 1.0 | 6 |
| 0.05 | 0.05 | 1.5 | 6 |

In all formulations, Pt catalyst = 1.0 wt % in the polymer.

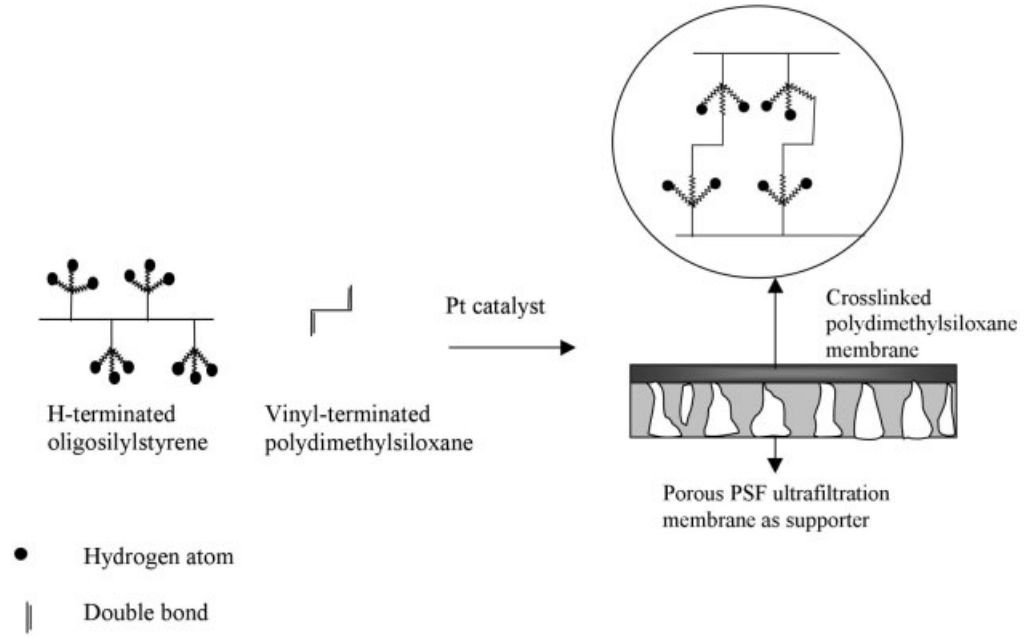


**Figure 2** Schematic illustration of the composite membranes prepared from oligo-$SiH_3$ and vinyl-PDMS.

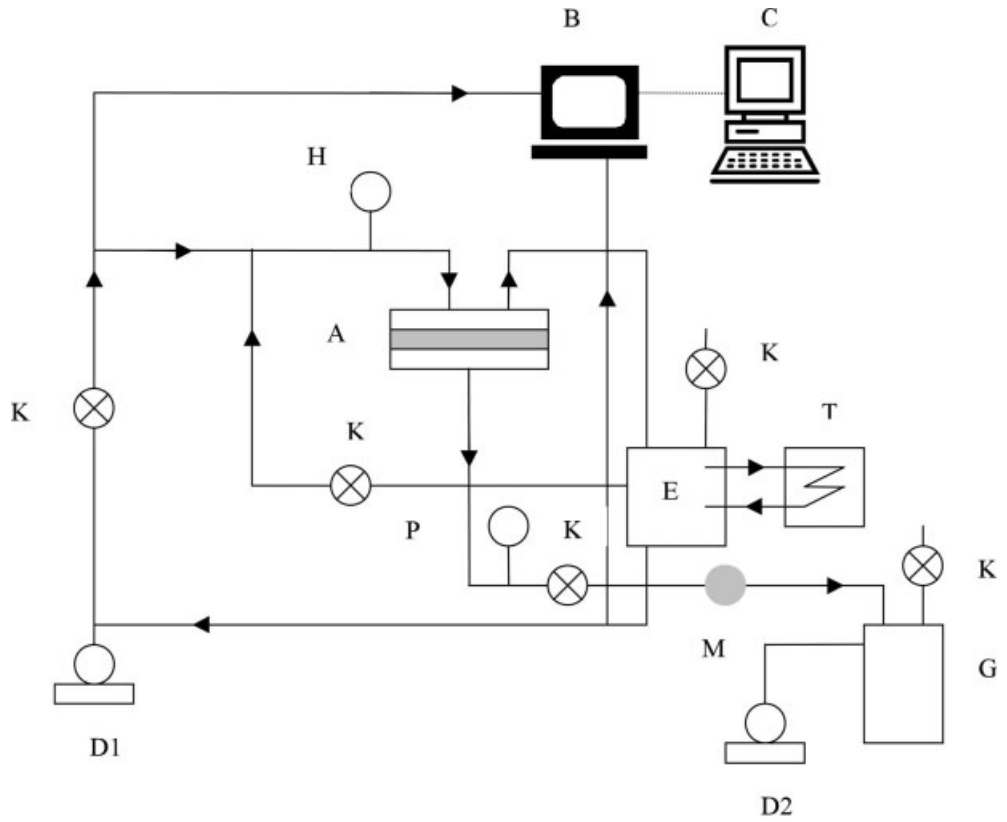


**Figure 3** Schematic diagram of the pervaporation apparatus: (A) pervaporation cell, (B) gas chromatograph, (C) computer, (D1) cycling pump, (D2) vacuum pump, (E) feed tank, (F) thermostat, (G) cold trap, (H) temperature transducer, (T) thermocouple, (P) pressure transducer, (M) mass flow meter, and (K) control valve.

**TABLE II**
**Effect of the Mass Ratio of Oligo-$SiH_3$ to Vinyl-PDMS on the Surface Properties of the Composite Membranes**

| Oligo-$SiH_3$/ vinyl-PDMS (mass ratio) | Viscosity of Vinyl-PDMS (cs) | | | | | |
|---|---|---|---|---|---|---|
| | 100 | 200 | 500 | 1,000 | 5,000 | 10,000 |
| 0.5 | S/R | S/R | S/R | S/R | S/R | S/R |
| 0.2 | S/R | S/R | S/R | S/R | S/R | S/R |
| 0.1 | St | St | S/R | S/R | S/R | S/R |
| 0.003 | St | St | St | St | St | St |

In all membranes, Pt catalyst = 1.0 wt % in the polymer; concentration of polymer in hexane = 20 wt %. S/R = membrane with a smooth and rubbery surface; St = membrane with a sticky surface.

curing, the membranes were moved to a 100°C oven for 8 h. The top layer thickness of the composite membranes was adjusted by the amount and concentration of the precursor solution poured onto the PSF membrane. The top layer thickness of the composite membranes was 39–550 $\mu$m; this was measured with a micrometer with an error range of $\pm 5$ $\mu$m.

### Pervaporation

Figure 3 shows the schematic diagram of the pervaporation apparatus. The membrane was clamped to the pervaporation cell, and the effective area of the membrane was 31.2 $cm^2$. The feed solution with 1,2-DCE was cycled by a pump, and the feed temperature was maintained with a water bath. The flow rate through the pervaporation cell was 0.35 L/min, corresponding to a Reynolds number of 97.[47] The pressure controller was used to monitor the change in the downstream pressure. The concentrations of the feed and the permeate vapor were analyzed with an HP 5890 gas chromatograph (Palo Alto, CA) equipped with Poropak P packed columns and a flame ionization detector. The pressure controller was used to check the pinholes in the top layer of the composite membranes. The permeation rate ($P$) was calculated from the amount of the solute ($Q_1$) or solvent ($Q_2$) through the effective membrane surface ($S$) at a given time ($t$):

$$P = Q_1(\text{or } Q_2)/(St) \quad (1)$$

The separation factor ($\alpha$) was calculated as follows:[34]

$$\alpha = (y_A/y_B)/(x_A/x_B) \quad (2)$$

where $x_A$ and $x_B$ are the molar fractions of 1,2-DCE and water in the feed, respectively, and $y_A$ and $y_B$ are the molar fractions of 1,2-DCE and water in the permeate, respectively. The permeation rate and separation factor were calculated with the data obtained after at least 3 h of separation once a steady state was achieved. The computer was used to record all operating parameters of the pervaporation process. The error ranges of the permeation rate and separation factor were 3 and 10%, respectively (95% confidence).

## RESULTS AND DISCUSSION

### Effect of the mass ratio of oligo-$SiH_3$ to vinyl-PDMS on the membrane performance

Table II lists the effects of the mass ratio of oligo-$SiH_3$ to vinyl-PDMS on the top layer morphology of the composite membranes. As shown in Table II, membranes with smooth and rubbery surface were obtained when

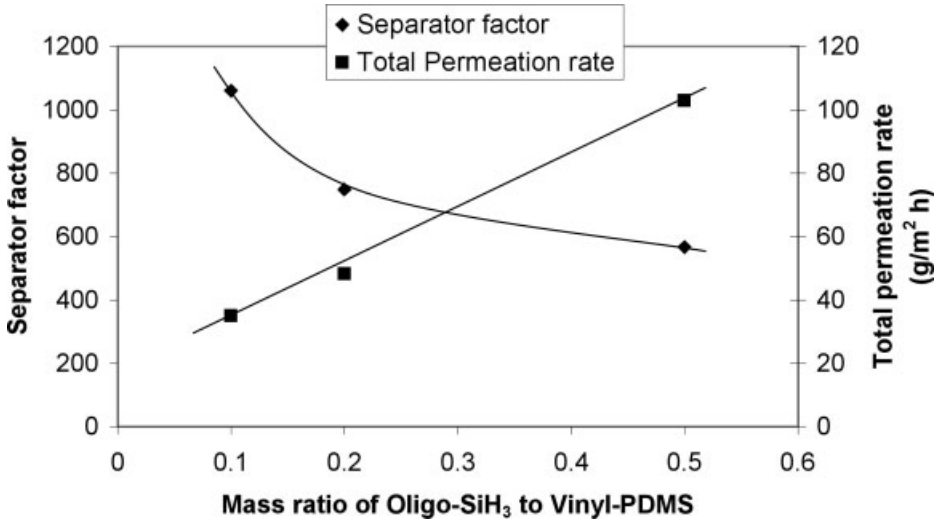


**Figure 4** Effect of the mass ratio of oligo-$SiH_3$ to vinyl-PDMS on the separation factor and total permeation rate (viscosity of vinyl-PDMS = 500 cs, thickness of the top layer = 56 $\mu$m, feed temperature = 25°C, downstream pressure = 5 Torr, feed solution = 100 ppm 1,2-DCE in water).

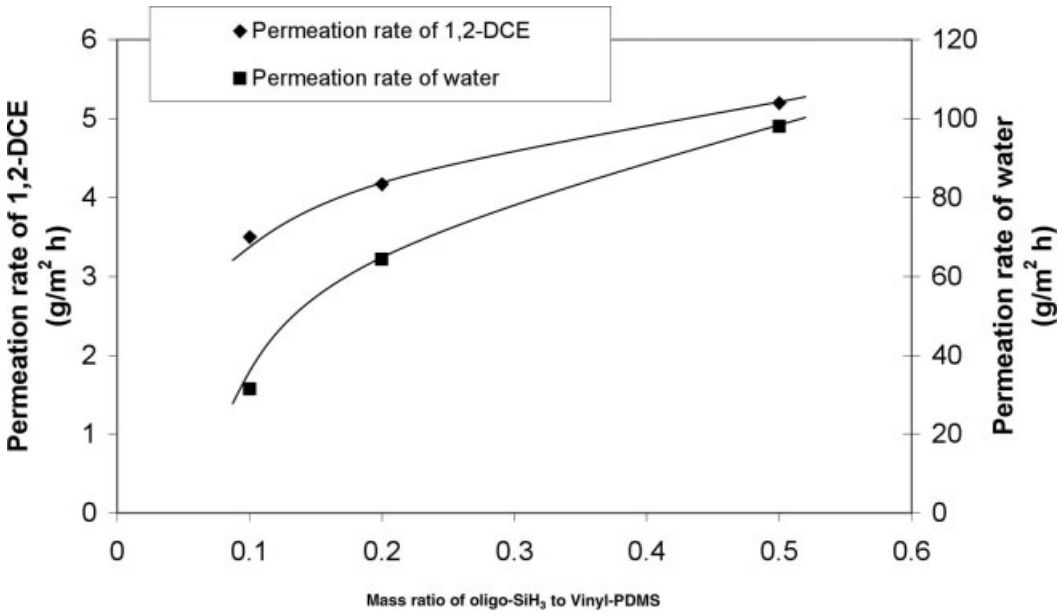


**Figure 5** Effect of the mass ratio of oligo-$SiH_3$ to vinyl-PDMS on the permeation rates of water and 1,2-DCE. The membranes are those presented in Figure 4 (feed temperature = 25°C, downstream pressure = 5 Torr, feed solution = 100 ppm 1,2-DCE in water).

the mass ratio of oligo-$SiH_3$ to vinyl-PDMS was greater than 0.2. A sticky surface was found when the mass ratio of oligo-$SH_3$ to vinyl-PDMS was less than 0.003. A sticky surface was also found when the mass ratio of oligo-$SH_3$ to vinyl-PDMS was 0.1 and vinyl-PDMS with a viscosity lower than or equal to 200 cs was used. An increase in the concentration of oligo-$SiH_3$ in the formulation accelerated the reaction rate of crosslinked PDMS and also increased the crosslinking density of the membranes. Therefore, membranes with smooth and rubbery surfaces as well as high mechanical strength could be achieved.[48] The sticky surface was generated when an inadequate crosslinking agent was used in the formulation. When the mass ratio of oligo-$SiH_3$ to vinyl-PDMS was kept constant, high-viscosity vinyl-PDMS was preferable for generating a crosslinking network with good

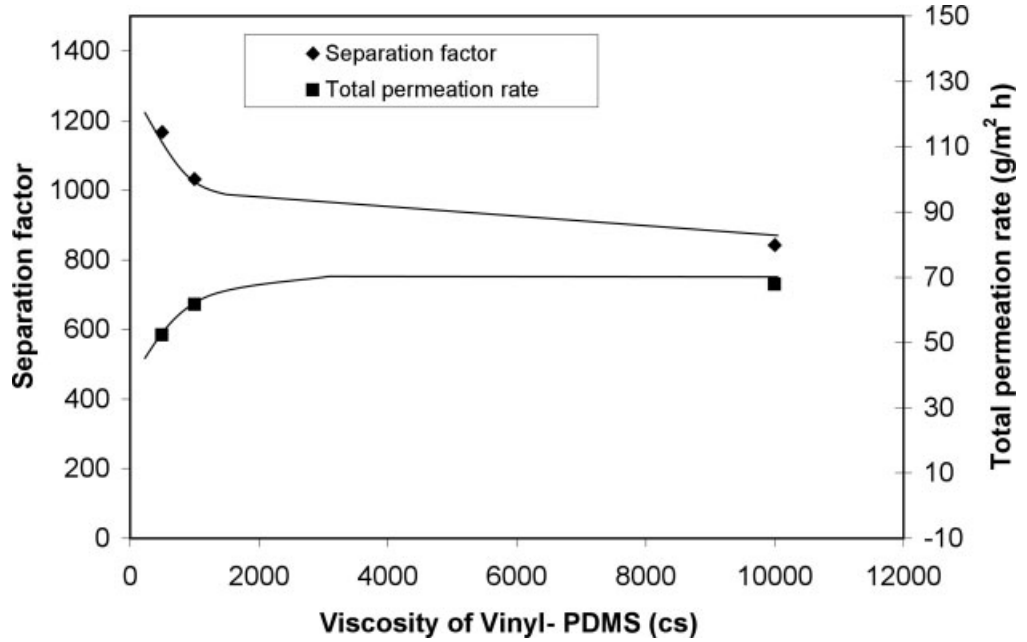


**Figure 6** Effect of the viscosity of vinyl-PDMS on the separation factor and total permeation rate (oligo-$SiH_3$/vinyl-PDMS mass ratio = 0.2, viscosity of vinyl-PDMS = 500 cs, thickness of the top layer = 70 $\mu$m, feed temperature = 25°C, downstream pressure = 5 Torr, feed solution = 100 ppm 1,2-DCE in water).

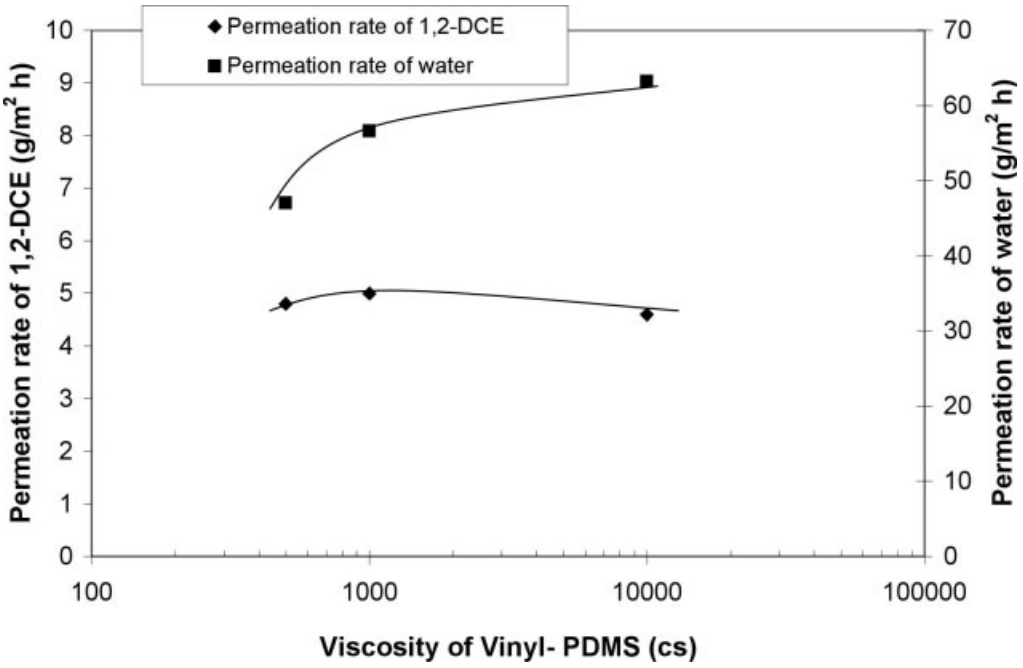


**Figure 7** Effect of the viscosity of vinyl-PDMS on the permeation rates of water and 1,2-DCE. The membranes are those presented in Figure 6 (feed temperature = 25°C, downstream pressure = 5 Torr, feed solution = 100 ppm 1,2-DCE in water).

mechanical strength. This was because vinyl-PDMS with a high viscosity represented a high molecular weight of PDMS, and so the mechanical strength of the prepared membranes was improved. Although there were no direct data for the mechanical strength and crosslinking density of the composite membranes, it was possible to judge the basic performance of the composite membranes from the morphology of the membrane surface because only the membranes with smooth and rubbery surfaces could be used as pervaporation membranes to achieve reasonable results.

Figure 4 shows the effect of the mass ratio of oligo-$SiH_3$ to vinyl-PDMS on the total permeation rate and separation factor. With an increasing mass ratio of

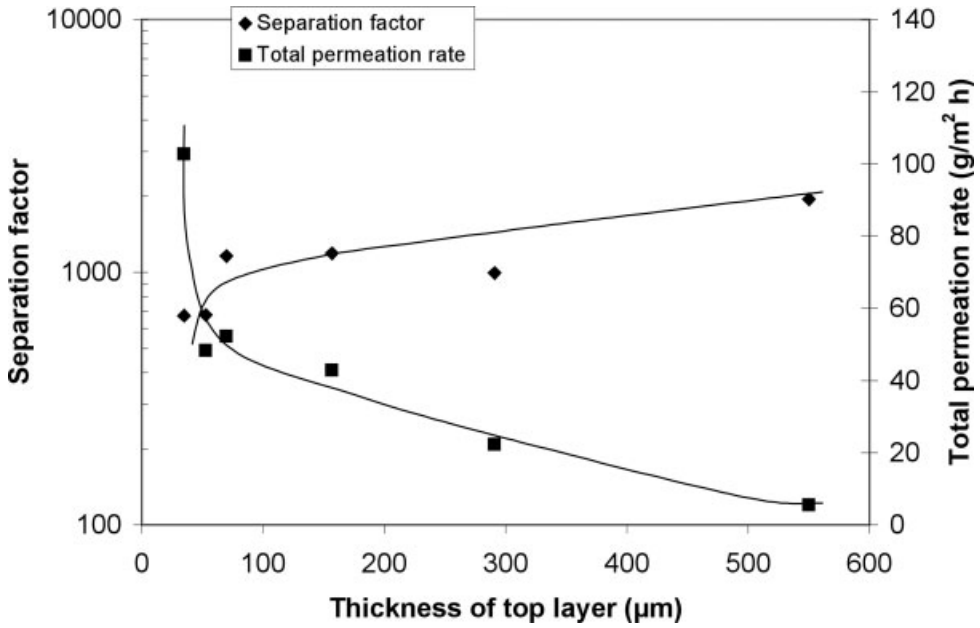


**Figure 8** Effect of the thickness of the top layer on the separation factor and total permeation rate (oligo-$SiH_3$/vinyl-PDMS mass ratio = 0.2, viscosity of vinyl-PDMS = 500 cs, feed temperature = 25°C, downstream pressure = 5 Torr, feed solution = 100 ppm 1,2-DCE in water).

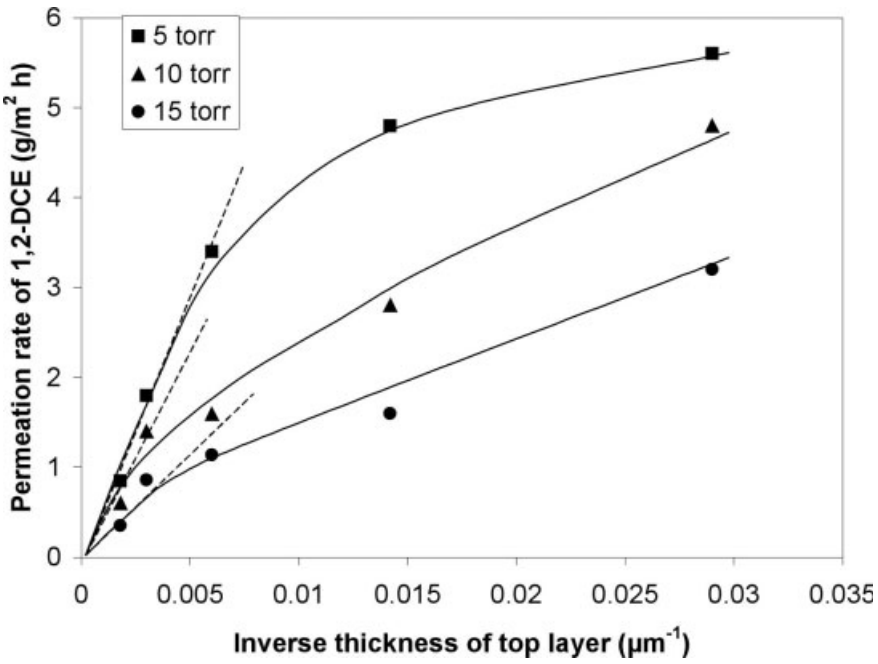


**Figure 9** Permeation rate of water versus the inverse thickness of the top layer. The membranes are those presented in Figure 8(feed temperature = 25°C, downstream pressure = 5 Torr, feed solution = 100 ppm 1,2-DCE in water).

oligo-$SiH_3$ to vinyl-PDMS, the total permeation rate increased, but the separation factor decreased. Vinyl-PDMS has an extremely flexible structure, and the polymer chains can be entangled with one another. Through the crosslinking of a PDMS network with oligo-$SiH_3$, the entangled PDMS chains can be separated, and enlarged interspaces among the polymer chains can be expected. The mass-transfer resistance through the membrane can be reduced as the interspaces among polymer chains increase. This is the reason that the total permeation rate increased. The reduction of the separation factor can be attributed to more water through the membrane than 1,2-DCE as the total permeation rate increased. Figure 5 shows the effect of the mass ratio of oligo-$SiH_3$ to vinyl-PDMS on the permeation rates of water and 1,2-DCE. The permeation rate of water increased more quickly than that of 1,2-DCE with an increasing mass ratio of oligo-$SiH_3$ to vinyl-PDMS.

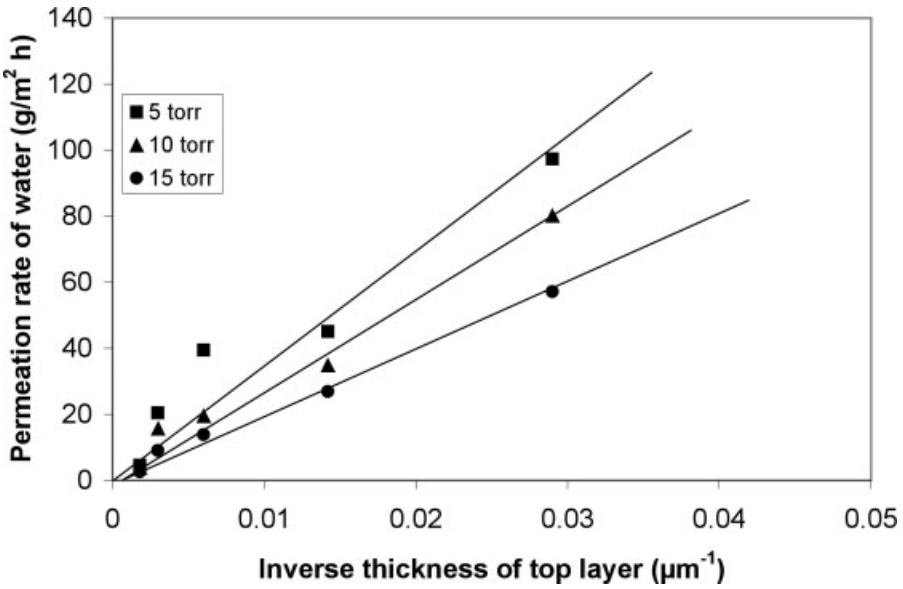


**Figure 10** Permeation rate of 1,2-DCE versus the inverse thickness of the top layer. The membranes are those presented in Figure 8 (feed temperature = 25°C, downstream pressure = 5 Torr, feed solution = 100 ppm 1,2-DCE in water).

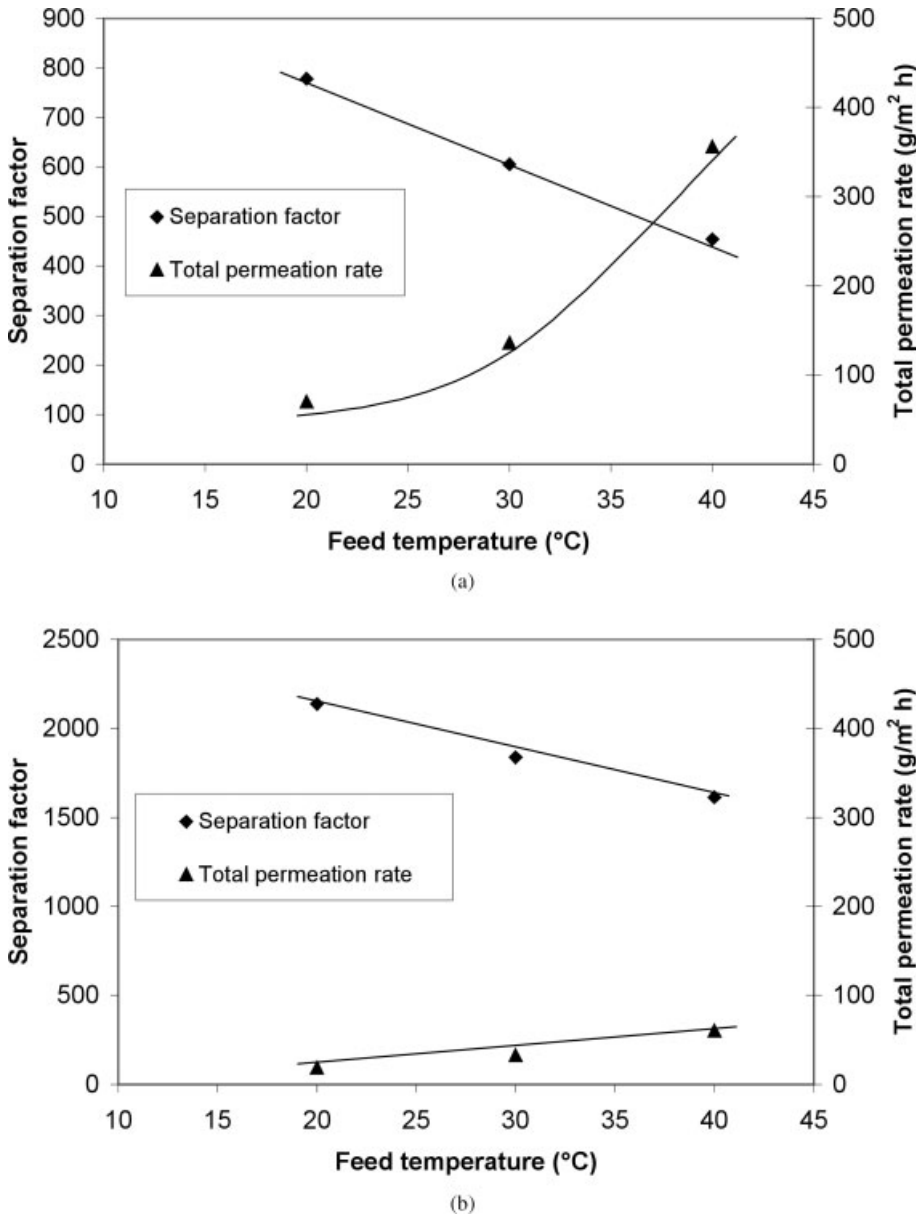


**Figure 11** Effect of the feed temperature on the separation factor and total permeation rate (oligo-$SiH_3$/vinyl-PDMS mass ratio = 0.2, viscosity of vinyl-PDMS = 500 cs, downstream pressure = 5 Torr, feed solution = 100 ppm 1,2-DCE in water): (a) top layer thickness = 35 $\mu$m and (b) top layer thickness = 157 $\mu$m.

### Effect of the viscosity of vinyl-PDMS on the membrane performance

Figure 6 shows the effect of the viscosity of vinyl-PDMS on pervaporation. When the viscosity of vinyl-PDMS was lower than 2000 cs, the total permeation rate increased, but the separation factor decreased with increasing viscosity. The crosslinking density of the composite membranes was expected to decreased when high-viscosity vinyl-PDMS was used. This is because vinyl-PDMS with a high viscosity has a longer chain structure. The longer the PDMS chains are, the looser the crosslinking networks are. This is the reason that the separation factor decreased and the permeation rate increased. The total permeation rate slightly increased and the separation factor slightly decreased when the viscosity of vinyl-PDMS was higher than 2000 cs. This may be the reason that the network properties of the polymer membranes reached their ultimate values with a further increase in the viscosity of vinyl-PDMS.[49] Figure 7 shows that the permeation rate of water increased, but the permeation rate of 1,2-DCE remained almost constant, as the viscosity of vinyl-PDMS increased.

### Effect of the top layer thickness on the membrane performance

Figure 8 presents the effect of the top layer thickness of the composite membranes on the total perme-

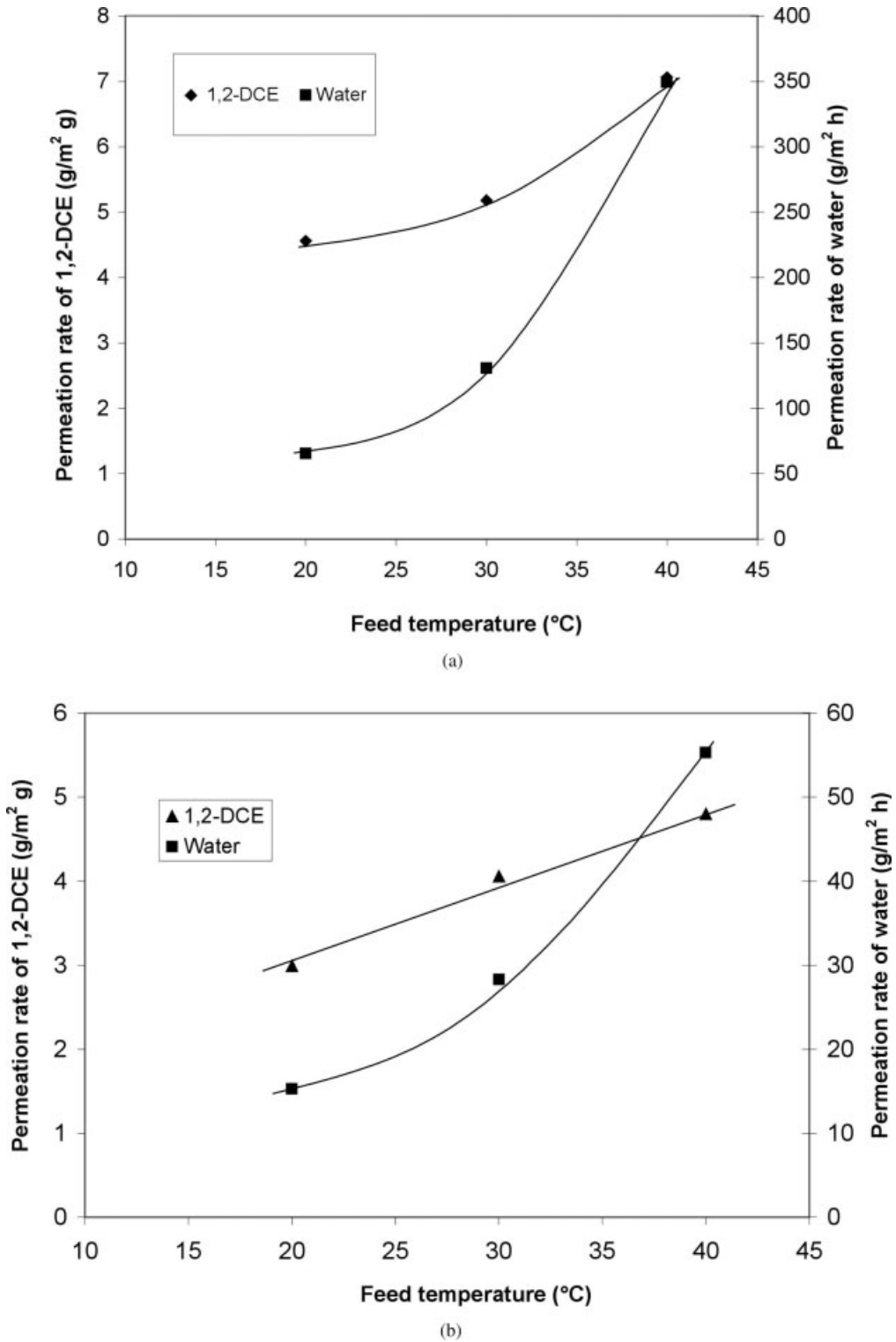


**Figure 12** Effect of the feed temperature on the permeation rates of water and 1,2-DCE. The membranes are those presented in Figure 11 (downstream pressure = 5 Torr, feed solution = 100 ppm 1,2-DCE in water): (a) top layer thickness = 35 $\mu$m and (b) top layer thickness = 157 $\mu$m.

ation rate and separator factor. With increasing top layer thickness, the total permeation rate decreased, but the separation factor increased. It is reasonable that the increase in the top layer thickness increased the total mass-transfer resistance. Therefore, the permeation rate deceased. The diffusion of water through the membranes became much difficult with increasing membrane thickness because of the hy-

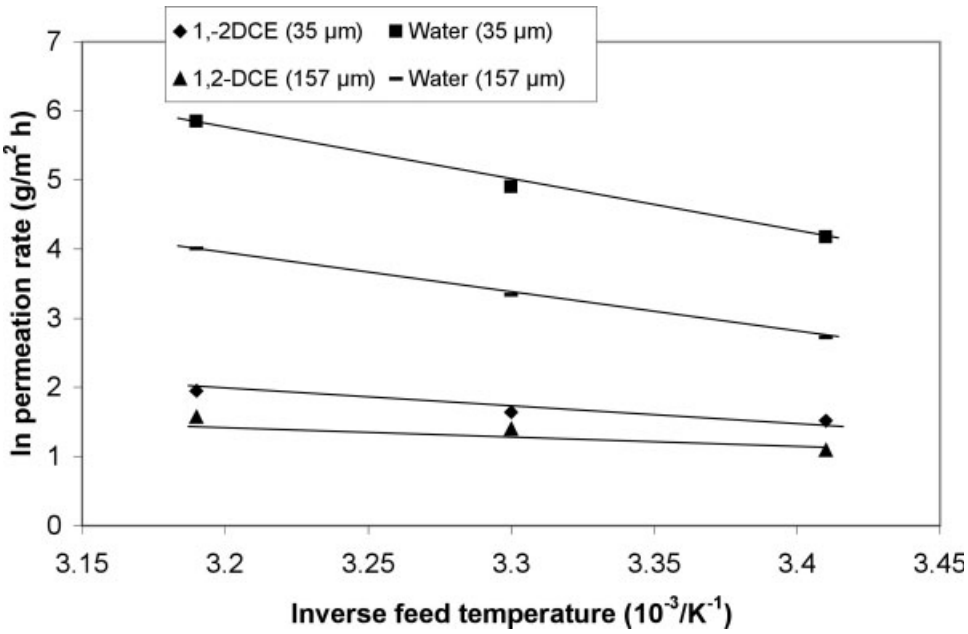


**Figure 13** Natural logarithm of the permeation rate versus the inverse feed temperature. The membranes are those presented in Figure 11 (downstream pressure = 5 Torr, feed solution = 100 ppm 1,2-DCE in water).

drophobic characteristics of the PDMS membranes. Consequently, the separation factor increased. The presence of a boundary layer could also influence the mass transfer of dichloroethane 1,2-dichloroethane (1,2-DCE), and the thicker membrane could effectively eliminate the effect of the boundary layer on the mass transfer of 1,2-DCE; therefore, both the permeation rate and separation factor of 1,2-DCE increased.

Figures 9 and 10 show the permeation rates of water and 1,2-DCE plotted as a function of the inverse top layer thickness at various downstream pressures. The permeation rate of 1,2-DCE was only linearly proportional to the inverse thickness for the thicker membrane, as indicated by the dotted line in Figure 9. There was a deviation of the permeation rate of 1,2-DCE from Fick's diffusion law[50] for the thinner membrane. The deviation could be attributed to the effect of the boundary layer on the mass-transfer process. It is well known that the boundary layer plays a critical role in the mass-transfer resistance for the pervaporation of VOCs.[51–53] Normally, two kinds of mass-transfer resistances exist in the pervaporation of VOCs. One is original from the intrinsic membrane, and another is from the boundary layer. The effect of the boundary layer is more significant on thinner membranes than on thicker membranes.[54] This is the reason that the thinner membrane showed obvious characteristics of deviation from Fick's diffusion law, as shown in Figure 9. Because the boundary layer had little effect on the transfer of water through the membrane, the permeation rates of water nearly followed Fick's diffusion law, as shown in Figure 10. Although the Reynolds number was lower (~97) in this study, the evaluation of the membrane performances by the compositions of the membranes and the operation conditions was still reasonable because we kept the Reynolds number constant for each measurement.

### Effect of the feed temperature

Figure 11 shows the effect of the feed temperature on the total permeation rate and separation factor for membranes with different top layer thicknesses. With an increasing feed temperature, the total permeation rate increased, but the separation factor decreased. This was because the frequency and amplitude of the PDMS chain motion increased at a higher feed temperature.[55] This could lead to a looser structure of the membranes. Therefore, the total permeation rate increased as the feed temperature increased. The reduction of the separation factor was the reason that more water could transfer through the membranes than 1,2-DCE when the

**TABLE III**
**Activation Energies of 1,2-DCE and Water**

| Thickness of the top layer ($\mu$m) | Activation energy (kcal/mol) | |
|---|---|---|
| | Water | 1,2-DCE |
| 35 | 12.3 | 2.8 |
| 157 | 14.2 | 3.8 |

The membranes are those in Figure 13; 1,2-DCE = 100 ppm in solution. The regression coefficients in Figure 13 were larger than 99%.

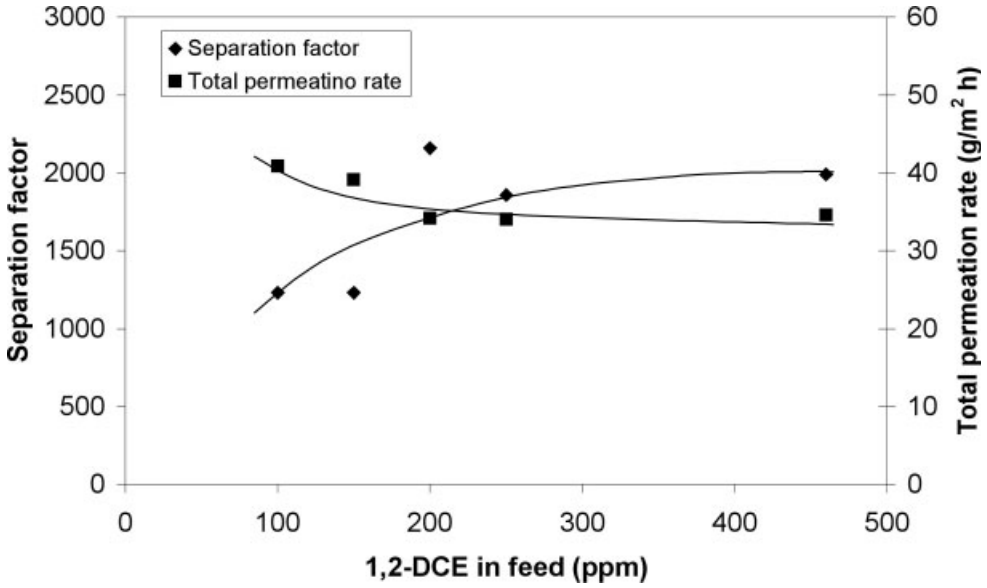


**Figure 14** Effect of the feed composition on the permeation rate and separation factor (oligo-$SiH_3$/vinyl-PDMS mass ratio = 0.2, viscosity of vinyl-PDMS = 500 cs, feed temperature = 25°C, downstream pressure = 5 Torr, thickness of the top layer = 70 $\mu$m).

feed temperature increased. Figure 12 shows that the permeation rates of water and 1,2-DCE increased with an increasing feed temperature for membranes with different thicknesses. Water had a faster permeation rate than 1,2-DCE. Figure 13 shows that an Arrhenius relationship exists between the permeation rate (both water and 1,2-DCE) and the feed temperature. The activation energies of water and 1,2-DCE through the membranes are listed in Table III. As expected, the activation energies of water and 1,2-DCE increased as the top layer thickness increased. Meanwhile, the activation energy of 1,2-DCE (2.8 or 3.8 kcal/mol) was lower than that of water (12.3 or 14.2 kcal/mol). This means that the composite membranes preferred to transfer 1,2-DCE.

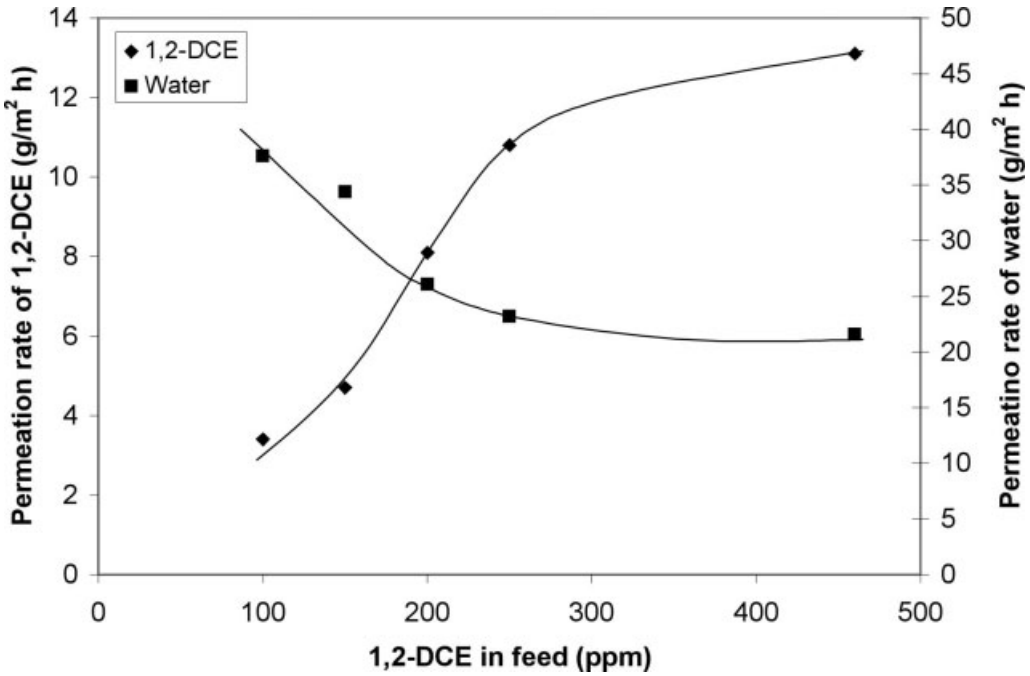


**Figure 15** Effect of the feed composition on the permeation rates of water and 1,2-DCE. The membranes are those presented in Figure 14 (feed temperature = 25°C, downstream pressure = 5 Torr).

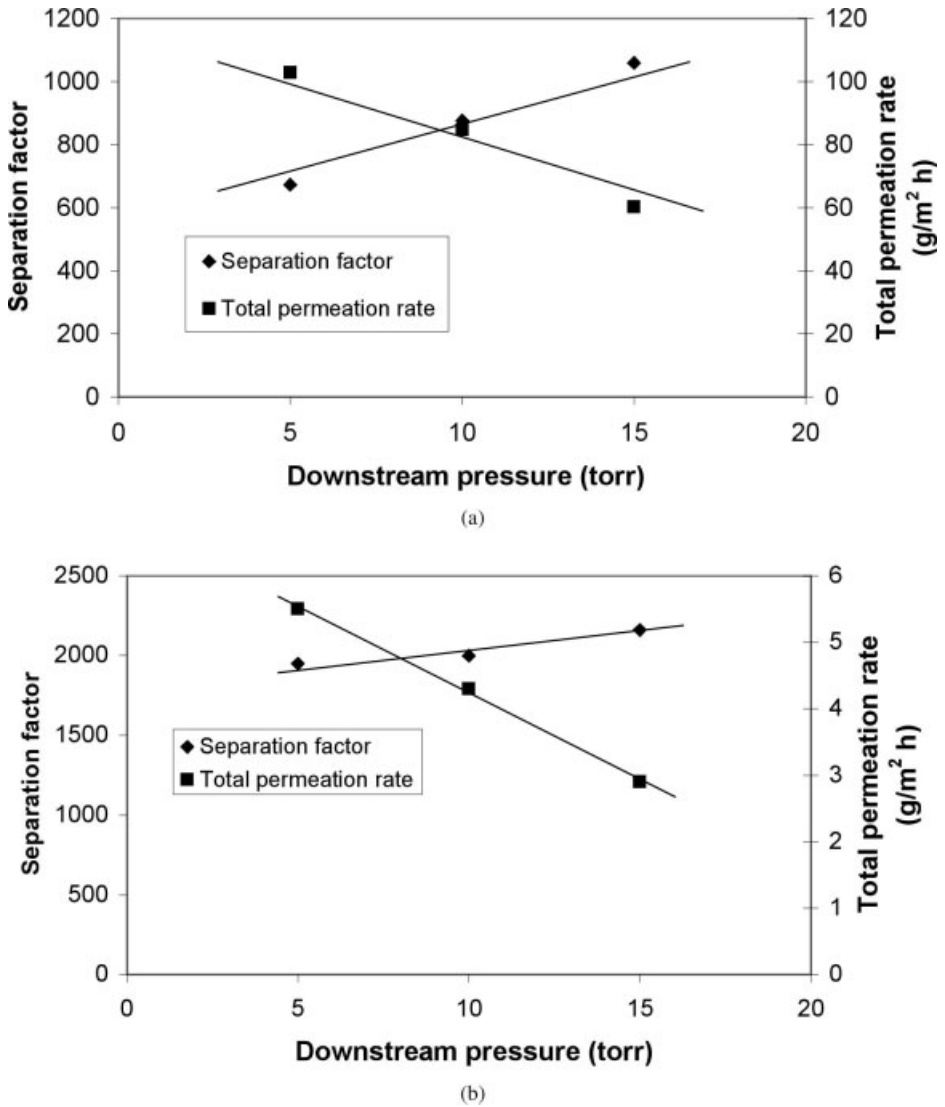


**Figure 16** Effect of the downstream pressure on the separation factor and total permeation rate (oligo-$SiH_3$/vinyl-PDMS mass ratio = 0.2, viscosity of vinyl-PDMS = 500 cs, feed temperature = 25°C, feed solution = 100 ppm 1,2-DCE in water): (a) top layer thickness = 35 $\mu$m and (b) top layer thickness = 550 $\mu$m.

### Effect of the feed composition

Figure 14 presents the total permeation rate and separation factor as a function of the feed composition. The total permeation rate decreased, but the separation factor increased, as the 1,2-DCE concentration increased in the feed. As the concentration of 1,2-DCE increased, the driving force of 1,2-DCE through the membranes increased. Therefore, more 1,2-DCE could be transferred through the membranes. The PDMS membranes were swollen as more 1,2-DCE was absorbed.[56] Although the resistance of mass transfer through the swollen membranes could be reduced, the swollen PDMS increased the hydrophobic property of the membranes, and this hindered the transfer of water, as shown in Figure 15. This is the reason that the separation factor increased with an increasing concentration of 1,2-DCE in the feed.

### Effect of the downstream pressure

Figure 16 shows the effect of the downstream pressure on the total permeation rate and separation factor for membranes with different thicknesses. With increasing downstream pressure, the separation factor increased, but the total permeation rate decreased. The driving force of permeation was proportional to the pressure difference between the feed and permeate side. The increase in the downstream pressure resulted in the reduction of the driving force, and the total permeation rate subsequently decreased. In comparison with the partial pressure of 1,2-DCE (78.9 Torr at 25°C),[57] the partial pressure of water in the feed mixture (23.5 Torr at 25°C)[58] was closer to the downstream pressure (5–15 Torr). The permeation rate of water was more sensitive to the variation of the down-

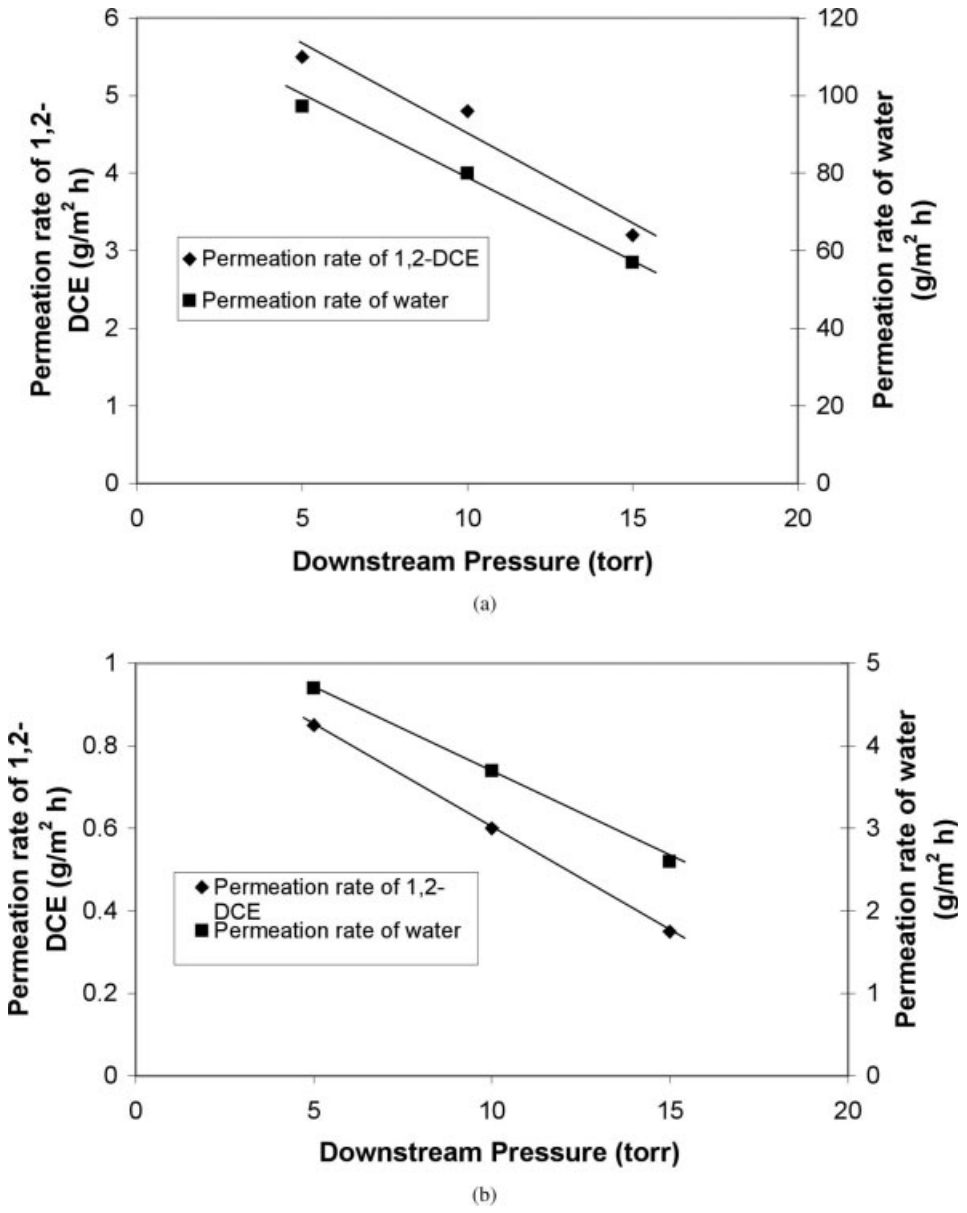


**Figure 17** Effect of the downstream pressure on the permeation rates of water and 1,2-DCE. The membranes are those presented in Figure 16 (feed temperature = 25°C, feed solution = 100 ppm 1,2-DCE in water): (a) top layer thickness = 35 $\mu$m and (b) top layer thickness = 550 $\mu$m.

stream pressure. Therefore, the permeation rate of water decreased more quickly than that of 1,2-DCE with increasing downstream pressure, as shown in Figure 17. A similar result was observed for the pervaporation of VOCs with organophilic membranes.[57]

## CONCLUSIONS

Novel PDMS membranes were prepared through the crosslinking of oligo-$SiH_3$ and vinyl-PDMS on the surface of a PSF ultrafiltration membrane with a platinum complex as the catalyst. A smooth and rubbery top layer was obtained when the mass ratio of oligo-$SiH_3$ to vinyl-PDMS was greater than 0.2. The composite membranes prepared from vinyl-PDMS with a viscosity of 500 cs and a mass ratio of oligo-$SiH_3$ to vinyl-PDMS of 0.2 demonstrated a compact structure and durable characteristics. The composite membranes were evaluated by the pervaporation of 1,2-DCE from dilute 1,2-DCE/water solutions. The activation energy of water through the membranes was almost 4 times higher than that of 1,2-DCE. The membrane showed the characteristics of preferential selection to 1,2-DCE, and the separation factor was 600–2300. A faster permeation rate of 1,2-DCE was achieved with increases in the feed temperature and feed concentration. On the other hand, the permeation rate of 1,2-DCE decreased with increases in the top layer thickness and

downstream pressure. The permeation rate of 1,2-DCE was 0.4–13 $g/m^2$ h; it depended on the membrane composition, top layer thickness, feed temperature, feed composition, and downstream pressure.

## References


1. Oliveira, T. A. C.; Scarpello, J. T.; Livingston, A. G. J Membr Sci 2002, 195, 75.
2. Qin, Y.; Sheth, J. P.; Sirkar, K. K. Ind Eng Res 2002, 41, 3413.
3. Dutta, B. K.; Sikdar, S. K. Environ Sci Technol 1999, 33, 1709.
4. Aminabhavi, T. M.; Khinnavar, R. S.; Harogoppad, S. R.; Aithal, U. S.; Nauyen, Q. T.; Hansen, K. C. J Macromol Chem Phys 1994, 34, 139.
5. Won, W.; Feng, X.; Lawless, D. J Membr Sci 2002, 209, 493.
6. Bluemke, W.; Schrader, J. Biomol Eng 2001, 17, 137.
7. Reyes, F. D.; Romero, J. M. F.; de Castro, M. D. L. Anal Chim Acta 2001, 434, 95.
8. Hernández, J. A.; de Castro, M. D. L. Food Chem 2000, 68, 387.
9. Pervaporation Membrane Separation Processes; Huang, R. Y. M., Ed.; Elsevier: New York, 1991; Chapter 10.
10. Miyata, T.; Higuchi, J.; Okuno, H.; Uragami, T. J Appl Polym Sci 1996, 61, 1315.
11. Schnabel, S.; Moulin, P.; Nguyen, Q. T.; Roizard, D.; Aptel, P. J Membr Sci 1998, 142, 129.
12. Hoshi, M.; Kobayashi, M.; Saitoh, T.; Higuchi, A.; Nakagawa, T. J Appl Polym Sci 1998, 69, 1483.
13. Miyata, T.; Takagi, T.; Kadota, T.; Uragami, T. Macromol Chem Phys 1995, 196, 1211.
14. Kim, H. J.; Nah, S. S.; Min, B. R. Adv Environ Res 2002, 6, 255.
15. Oh, H. K.; Song, K. H.; Lee, K. R.; Rim, J. M. Polymer 2001, 42, 6305.
16. Shepherd, A.; Habert, A. C.; Borges, C. P. Desalination 2002, 148, 111.
17. Wu, P.; Field, R. W.; Brisdon, B. J.; England, R.; Barkley, S. J. Sep Purif Technol 2001, 22, 339.
18. Yeow, M. L.; Field, R. W.; Li, K.; Teo, W. K. J Membr Sci 2002, 203, 137.
19. Bell, C. M.; Gerner, F. J.; Strathmann, H. J Membr Sci 1988, 36, 315.
20. Arkles, B. CHEMTECH 1983, 13, 542.
21. Okamoto, K.; Butsuen, A.; Tsuru, S.; Nishioka, S.; Tanaka, K.; Kita, H.; Asakawa, S. Polym J 1987, 19, 734.
22. Akiyama, E.; Takamura, Y.; Nagaze, Y. Makromol Chem 1992, 193, 1509.
23. Takegaemi, S.; Yamada, H.; Tsujii, S. J Membr Sci 1992, 75, 93.
24. Liang, L.; Ruckenstein, E. J Membr Sci 1996, 114, 227.
25. Uragami, T.; Yamada, H.; Miyata, T. J Membr Sci 2001, 187, 255.
26. Schauer, J.; Sysel, P.; Maroušek, V.; Pientka, Z.; Pokorn, J.; Bleha, M. J Appl Polym Sci 1998, 61, 1333.
27. Mishima, S.; Nakagawa, T. J Appl Polym Sci 1999, 73, 1835.
28. Nguyen, Q. T.; Bendjama, Z.; Clement, R.; Ping, Z. Phys Chem 2000, 2, 395.
29. Vankelecom, I. F. J.; Moremans, B.; Jacobs, P. A.; Beuckelaer, W. D.; Martens, J. A.; Ravishankar, R. Chem Commun 2000, 24, 2467.
30. Brook, M. A.; Hulser, P.; Sebastian, T. Macromolecules 1989, 22, 3814.
31. Mark, H.; Bikales, N. M.; Overberger, C. G.; Menges, G. Encyclopedia of Polymer Science and Engineering; Wiley: New York, 1985; p 558.
32. Yeom, C. K.; Dickson, J. M.; Brook, M. A. Korean J Chem Eng 1996, 13, 482.
33. Brook, M. A.; Modi, P.; Dickson, J. M. Macromolecules 1993, 26, 2624.
34. Lau, W. W. Y.; Finlayson, J.; Dickson, J. M.; Jiang, J. X.; Brook, M. A. J Membr Sci 1997, 134, 209.
35. Horvath, A. L. Halogenated Hydrocarbons: Solubility–Miscibility with Water; Marcel Dekker: New York, 1982.
36. Howard, P. H. Handbook of Environmental Rate and Exposure Data for Organic Chemicals; Lewis: Chelsea, MI, 1990.
37. Class, T.; Ballschmiter, K. Fresenius J Anal Chem 1987, 327, 198.
38. Klecka, G. M.; Carpenter, C. L.; Gonsior, S. J. J Contam Hydrol 1998, 34, 139.
39. Wycisk, P.; Weiss, H.; Kaschl, A.; Heidrich, S.; Sommerwerk, K. Toxicol Lett 2003, 140, 343.
40. Khayet, M.; Matsuura, T. Desalination 2002, 148, 31.
41. Dotremont, C.; Brabants, B.; Geeroms, K.; Mewis, J.; Vandecasteele, C. J Membr Sci 1995, 104, 109.
42. Dutta, B. K.; Sikdar, S. K. Environ Sci Technol 1999, 33, 1709.
43. Pereira, C. C.; Habert, A. C.; Nobrega, R.; Borges, C. P. J Membr Sci 1998, 138, 227.
44. Baker, R. W.; Wijmans, J. G.; Athayde, A. L.; Daniels, R.; Ly, J. H.; Le, M. J Membr Sci 1997, 137, 159.
45. Ji, W.; Hilaly, A.; Sikdar, S. K.; Hwang, S. T. J Membr Sci 1994, 97, 109.
46. Athayde, A. L.; Baker, R. W.; Daniels, R.; Le, M. H.; Ly, J. H. CHEMTECH 1997, 27, 34.
47. Moller, P. S. J Basic Eng 1966, 67, 155.
48. Odian, G. Principles of Polymerization; Wiley: New York, 1991; Chapter 2.
49. Sperling, L. H. Introduction to Physical Polymer Science; Wiley: New York, 1992; Chapter 1.
50. Atkins, P. W. Physical Chemistry; Freeman: New York, 1985; Chapter 26.
51. Psaume, R.; Aptel, P.; Aurelle, Y.; Mora, J. C.; Bersillon, J. L. J Membr Sci 1988, 36, 373.
52. Nijhuis, H. H.; Mulder, M. H. V.; Smolders, C. A. J Membr Sci 1991, 61, 99.
53. Raghunath, B.; Hwang, S. T. J Membr Sci 1992, 65, 147.
54. Karlsson, H. O. E.; Trägårdh, G. J Membr Sci 1993, 81, 163.
55. Huang, R. Y. M.; Yeom, C. K. J Membr Sci 1990, 51, 273.
56. Lamer, T.; Rohart, M. S.; Voilley, A.; Baussart, H. J Membr Sci 1994, 90, 251.
57. Ji, W. C.; Sikdar, S. K.; Hwang, S. T. J Membr Sci 1994, 93, 1.
58. Daubert, T. E.; Danner, R. P.; Sibul, H. M.; Stebbins, C. C. Physical and Thermodynamic Properties of Pure Chemicals; Taylor & Francis: Washington, DC, 1995.